

DUST PRODUCTION AND MASS LOSS IN THE GALACTIC GLOBULAR CLUSTER NGC 362

MARTHA L. BOYER¹, IAIN McDONALD², JACCO TH. VAN LOON², KARL D. GORDON¹, BRIAN BABLER³, MIWA BLOCK⁴, STEVE BRACKER³, CHARLES ENGELBRACHT⁴, JOE HORA⁵, REMY INDEBETOUW⁶, MARILYN MEADE³, MARGARET MEIXNER¹, KARL MISSELT⁴, JOANA M. OLIVEIRA², MARTA SEWIL¹, BERNIE SHIAO¹, AND BARBARA WHITNEY¹

(Received; Revised; Accepted)
Draft version May 28, 2018

ABSTRACT

We investigate dust production and stellar mass loss in the Galactic globular cluster NGC 362. Due to its close proximity to the Small Magellanic Cloud (SMC), NGC 362 was imaged with the IRAC and MIPS cameras onboard the *Spitzer Space Telescope* as part of the Surveying the Agents of Galaxy Evolution (SAGE-SMC) *Spitzer* Legacy program. We detect several cluster members near the tip of the Red Giant Branch that exhibit infrared excesses indicative of circumstellar dust and find that dust is not present in measurable quantities in stars below the tip of the Red Giant Branch. We modeled the spectral energy distribution (SED) of the stars with the strongest IR excess and find a total cluster dust mass-loss rate of $3.0_{-1.2}^{+2.0} \times 10^{-9} M_{\odot} \text{ yr}^{-1}$, corresponding to a gas mass-loss rate of $8.6_{-3.4}^{+5.6} \times 10^{-6} M_{\odot} \text{ yr}^{-1}$, assuming $[\text{Fe}/\text{H}] = -1.16$. This mass loss is in addition to any dust-less mass loss that is certainly occurring within the cluster. The two most extreme stars, variables V2 and V16, contribute up to 45% of the total cluster dust-traced mass loss. The SEDs of the more moderate stars indicate the presence of silicate dust, as expected for low-mass, low-metallicity stars. Surprisingly, the SED shapes of the stars with the strongest mass-loss rates appear to require the presence of amorphous carbon dust, possibly in combination with silicate dust, despite their oxygen-rich nature. These results corroborate our previous findings in ω Centauri.

Subject headings: globular clusters: individual (NGC 362) – stars: mass loss – circumstellar matter – stars:winds, outflows – infrared: stars – stars: AGB and post-AGB

1. INTRODUCTION

Stellar mass loss and dust production remain two of the most critical, yet least understood, aspects of stellar evolution models, especially in low-mass population II stars. High-mass Asymptotic Giant Branch (AGB) stars (up to $8 M_{\odot}$) evolve and lose mass on very short timescales, resulting in short bursts of dust input into the Interstellar Medium (ISM) following episodes of star formation. Low-mass stars are more numerous than their high-mass counterparts and live much longer, resulting in a more sustained dust input into the ISM. Constraining these aspects is crucial for determining the impact of low-mass stars – the most numerous stars in the Universe – on galaxy evolution. Observations with the *Spitzer Space Telescope* (Werner et al. 2004; Gehrz et al. 2007) and the *AKARI* telescope (Murakami et al. 2007) have produced many studies of infrared photometry of resolved stellar populations in globular clusters (GCs). Despite these new studies, the sample of observations is still quite small, consisting of only a handful of GCs and creating almost as many new questions as it has answered.

Origlia et al. (2007) argued on the basis of their analysis of *Spitzer* data for 47 Tuc that dust-accompanied mass loss occurs along the entire Red Giant Branch (RGB), down to the Horizontal Branch (HB). However, this was not confirmed with *AKARI* observations (Ita et al. 2007). In other GCs, dusty mass loss is only seen near the very tip of the RGB (Boyer et al. 2008; McDonald et al. 2009).

Intracluster dust clouds should form as a result of dusty mass loss from many stars during the time between Galactic plane crossings. Searches for this dust in a large sample of GCs using *Spitzer* and *AKARI* have resulted in no successful/significant detections (Barmby et al. 2009; Matsunaga et al. 2008), with the exception of M15 (Boyer et al. 2006). This lack of intracluster medium (ICM) dust in most clusters provides a mystery as to the fate of dust produced by evolved stars in GCs.

1.1. NGC 362

We present an infrared study of NGC 362, a bright GC in the southern sky. As one half of the classical “second-parameter” GC pair with NGC 288, NGC 362 is a relatively well-studied cluster (e.g., Bellazzini et al. 2001; Catelan et al. 2001). The wide availability of multi-wavelength and astrometric data, along with the cluster’s large coeval stellar population, a metallicity intermediate to 47 Tuc and the bulk population of ω Cen ($[\text{Fe}/\text{H}] = -1.16$ for NGC 362, Harris 1996)⁷, and proximity to us (8.5 kpc, Harris 1996) make it an ideal candidate for a study of dusty mass loss on the AGB and upper RGB.

¹ STScI, 3700 San Martin Drive, Baltimore, MD 21218 USA; mboyer@stsci.edu

² Astrophysics Group, Lennard-Jones Laboratories, Keele University, Staffordshire ST5 5BG, UK

³ Department of Astronomy, University of Wisconsin, Madison, 475 North Charter Street, Madison, WI 53706-1582 USA

⁴ Steward Observatory, University of Arizona, 933 North Cherry Avenue, Tucson, AZ 85721 USA

⁵ Harvard-Smithsonian Center for Astrophysics, 60 Garden Street, MS 65, Cambridge, MA 02138-1516 USA

⁶ Department of Astronomy, University of Virginia, P.O. Box 3818, Charlottesville, VA 22903-0818 USA

⁷ The Harris (1996) catalog was update in February 2003. See <http://www.physwww.physics.mcmaster.ca/~harris/mwgc.dat>

TABLE 1
NGC 362 PROPERTIES

Parameter	Value	Source
Right Ascension (J2000)	01 ^h 03 ^m 14 ^s .27	
Declination (J2000)	-70°50′53″.6	
Distance (kpc)	8.5	3
[Fe/H]	-1.16	3
M (M_{\odot})	3.78×10^5	2
R_{core} (′)	0.17	3
$R_{\text{half mass}}$ (′)	0.81	3
$E(B - V)$ (mag)	0.05	3
$(m - M)_V$	14.65	3
τ_c (yr) ^a	3×10^7	4
N_{HB}	1.6×10^2	1
$v_{\text{esc},0}$ (km s ⁻¹) ^b	46.7	5
M_V (mag)	-8.35	3
L_{bol} (L_{\odot})	4.54×10^5	3
Heliocentric radial velocity (km s ⁻¹)	223.5 ± 0.5	3

NOTE. — Sources: (1) Barmby et al. (2009), (2) Gnedin & Ostriker (1997), (3) Harris (1996), (4) Odenkirchen et al. (1997), (5) McLaughlin & van der Marel (2005).

^a τ_c is the time since the last Galactic plane-crossing.

^b $v_{\text{esc},0}$ is the escape velocity at $R = 0$.

Compared to NGC 288, NGC 362 has a red HB, despite having a very similar metallicity to the former (i.e., the “first parameter”). There are several theories for this discrepancy, including (and possibly combining) cluster age, helium abundances, and RGB mass loss, which may be affected by the central concentration of the cluster or other environmental factors (Catelan et al. 2001). A recent study also suggests environmental conditions during formation as a second-parameter candidate (Fraix-Burnet et al. 2009).

NGC 362 appears to be devoid of an ICM. Barmby et al. (2009) find an upper limit of $6.3 \times 10^{-5} M_{\odot}$ of dust, more than two orders of magnitude less than predicted based on the number of HB stars and the time since the last Galactic plane-crossing (τ_c , see Table 1). In addition, Grindlay & Liller (1977) and Hesser & Shawl (1977) searched for and found no ionized intracluster medium. Despite the apparent lack of material collected from mass-losing stars in the cluster, two studies have identified a small population of sources with infrared excesses attributed to circumstellar dust and mass loss (Origlia et al. 2002; Ita et al. 2007), and McDonald & van Loon (2007) have identified cluster stars with H α profiles that indicate mass loss in the absence of dust.

2. OBSERVATIONS AND DATA REDUCTION

A 3-color image composed of 3.6, 8, and 24 μm Infrared Array Camera (IRAC) and Multiband Imaging Photometer (MIPS) images of NGC 362 is presented in Figure 1. The cluster’s near-juxtaposition with the Small Magellanic Cloud (SMC) resulted in serendipitous observations of NGC 362 with *Spitzer* as part of the Surveying the Agents of Galaxy Evolution *Spitzer* Legacy Program (SAGE-SMC; K.D.Gordon 2009, in preparation). NGC 362 lies approximately 2° north from the center of the SMC bar, placing it near the edge of our 5° × 5° *Spitzer* observations. The cluster was covered at 3.6, 4.5, 5.8, 8, 24, and 70 μm to well outside of its half-mass ra-

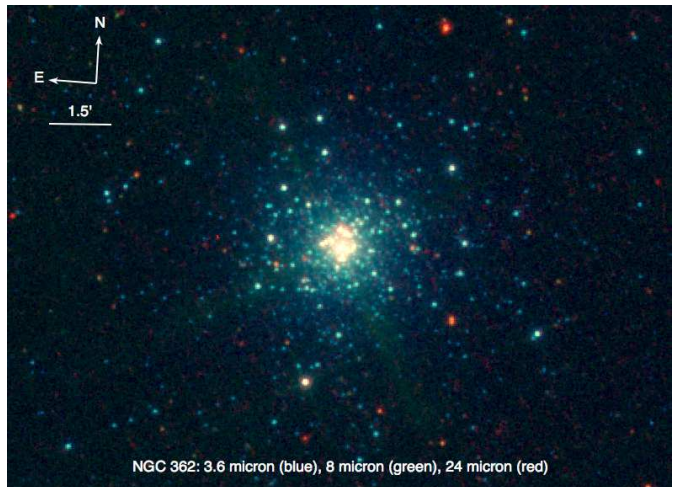


FIG. 1.— 3-color IRAC and MIPS image of NGC 362. Blue is 3.6 μm , green is 8 μm , and red is 24 μm . The northern most portion of the SMC bar lies approximately 1° to the south.

dius of 0.81′ (Harris 1996). SAGE-SMC 160 μm images did not include the cluster. All data and analysis presented here are confined to within 6′ of the cluster center to minimize contamination from SMC sources.

Observations consist of two epochs of IRAC images separated by 3 months and one epoch of MIPS images. The 1 σ sensitivities are 2.3, 3.4, 19.1, 20.5, and 28.1 μJy for 3.6, 4.5, 5.8, 8, and 24 μm , respectively. Short exposure times (12 s) ensure that saturation of cluster stars is not an issue. Angular resolutions for IRAC wavelengths range from 1.7″ at 3.6 μm to 1.9″ at 8 μm and increase to 5.8″ for MIPS 24 μm . For more details regarding data acquisition and reduction for the SAGE-SMC program, see K.D.Gordon, et al. (2009, in preparation).

Photometry should be reasonably complete to well beyond the HB ($M_{\text{HB}} \approx -1$ mag at 3.6 μm), as demonstrated by a steady increase in source counts to $M_{3.6\mu\text{m}} \approx 2$ mag in Figure 2. While photometric completeness tests have not yet been performed on the SAGE-SMC data, the completeness limits beyond the crowded inner 1′ of the cluster are likely similar to those for the SAGE Large Magellanic Cloud (SAGE-LMC) IRAC data (Meixner et al. 2006) since the observations were similarly designed. At 3.6 μm , the average photometric completeness limit for SAGE-LMC is ≈ 16 mag ($M_{3.6\mu\text{m}} \approx 1.4$ mag for NGC 362). The luminosity function in the inner 1′ of the cluster is truncated just below the HB (Fig. 2); this is a result of incompleteness due to crowding. The fact that the luminosity function at brighter levels does not differ in the cluster core from the field means that crowding is not important for stars brighter than the HB.

Only three point sources are detected at 70 μm , and only one of these (designated here as s11) is also detected in IRAC. This source is discussed further in Section 3.2.

2.1. Ancillary Data

To aid in estimating the temperatures and luminosities of the cluster stars, we collected literature photometry spanning the optical and the near-IR. NGC 362 was observed in the Magellanic Clouds Photometric Survey (MCPS; Zaritsky et al. 2002), the Deep Near-Infrared Southern Sky Survey (DENIS; Epchtein et al. 1997), the

Naval Observatory Merged Astrometric Dataset (NO-MAD; Zacharias et al. 2005) and the Two Micron All Sky Survey (2MASS; Skrutskie et al. 2006).

The MCPS catalog includes UBVI photometry, but does not cover the inner $\approx 0.3'$ of the cluster core, where four candidate mass-losing stars identified with *Spitzer* data reside (see Section 3). We obtained optical photometry of stars in the cluster core from the DENIS and Nomad catalogs, which include I -, J -, and K_s -band photometry and B -, V -, and R -band photometry, respectively. 2MASS includes JHK_s photometry and probes to the cluster center. This collection of optical and near-IR data complements the $3.6 \mu\text{m}$ *Spitzer* data in both completeness and angular resolution, with 93% of the $3.6 \mu\text{m}$ sources matched in at least one of these four ancillary catalogs. The remaining 7% of $3.6 \mu\text{m}$ sources without optical or near-IR counterparts have a mean $3.6 \mu\text{m}$ magnitude of 16.5 mag, with a standard deviation of 1.3 mag, or three magnitudes fainter than the HB. All of the sources investigated in detail in this study (Section 3) are detected in at least one near-IR or optical catalog.

In addition, Ita et al. (2007) obtained infrared photometry at 2.4, 3.2, 4.1, 7.0, 9.0, 11.0, 15.0, 18.0, and $24 \mu\text{m}$ with the Infrared Camera (IRC; Onaka et al. 2007) onboard the *AKARI* telescope (see Fig. 3 from Ita et al. 2007, photometry obtained through private communication). IRC images have angular resolutions ranging from $0.9''$ at $2.4 \mu\text{m}$ to $9''$ at $24 \mu\text{m}$, making stellar blending a problem in the most crowded regions of the cluster.

NGC 362 was also observed at 24 and $70 \mu\text{m}$ by Barmby et al. (2009). While none of the candidate mass-losing stars identified in Section 3 are detected at $70 \mu\text{m}$, the supplementary $24 \mu\text{m}$ data are useful for estimating dust compositions and mass-loss rates of individual stars (see Section 3.5).

A Hubble ACS image was obtained with permission from the ACS Survey of Galactic globular clusters team (Sarajedini et al. 2007). The high resolution of this image was helpful in determining when stellar blending in *Spitzer* and *AKARI* images is potentially a problem.

2.2. Cluster Membership

Proper motions in NGC 362 were obtained by Zacharias et al. (2005) and Tucholke (1992). The latter computed a membership likelihood by fitting the distribution of stars in $\mu_\alpha \cos \delta$, μ_δ space with a sum of two bivariate Gaussians representing NGC 362 and field stars. We use these probability estimates to eliminate non-members. For proper motions from Zacharias et al. (2005), we employ a conservative cut-off of $>35 \text{ mas yr}^{-1}$ to eliminate probable cluster non-members.

The heliocentric radial velocity (v_{rad}) of NGC 362 is $223.5 \pm 0.5 \text{ km s}^{-1}$ (Harris 1996). Fischer et al. (1993) measured radial velocity for 215 stars around the center of the cluster, and confirmed two stars in their sample as radial velocity non-members. Harris & Zaritsky (2006) measure the radial velocities of red giants in the SMC as $146 \pm 28 \text{ km s}^{-1}$, and find that it is rare for an SMC star to have a radial velocity larger than 200 km s^{-1} . However, they did not measure stars at positions near NGC 362, and we therefore note that it is possible, although rare, for SMC stars to have radial velocities sim-

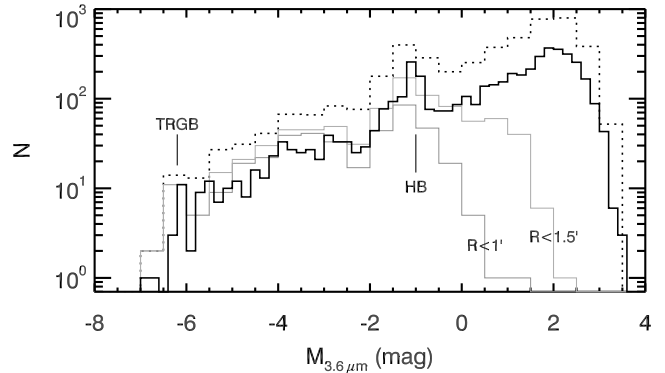


FIG. 2.— Luminosity function of NGC 362 (within $R = 6'$), including both epochs of IRAC data. The solid and dotted lines illustrate 0.2 and 0.5 magnitude bins, respectively. The tip of the Red Giant Branch (TRGB) is located near $M_{3.6\mu\text{m}} \approx -6.2$ mag, and the Horizontal Branch (HB) is located near $M_{3.6\mu\text{m}} \approx -1.0$ mag. Photometry should be reasonably complete to approximately 3 magnitudes fainter than the HB at $3.6 \mu\text{m}$. In the inner $1'$ of the cluster (gray line) crowding limits source completeness to magnitudes brighter than the HB.

ilar to NGC 362 due to the rotation of the SMC (for relatively high-mass stars) and its velocity dispersion (in particular for low-mass stars).

Membership information is available for 68% of the sources detected by *Spitzer*. We suspect that many of the sources without membership information (especially those with extreme IR excess) are in fact background galaxies that are not detected in the optical (see Section 3.2).

3. MASS-LOSING STARS IN NGC 362

3.1. Previously Identified Mass-Losing Stars

Three sources in NGC 362 (designated as x01, x02, and x03 by McDonald & van Loon 2007) were identified as having infrared excess by Origlia et al. (2002) using $12\text{-}\mu\text{m}$ *Infrared Space Observatory (ISO)* data. The coordinates of source x01 coincide with a *Spitzer* source that shows $24 \mu\text{m}$ excess (source s04, see Table 2). McDonald & van Loon (2007) showed x01 to have a red $\text{H}\alpha$ line emission wing and blue-shifted line absorption core, indicative of an outflow with a mass-loss rate of $\sim 10^{-6} M_\odot \text{ yr}^{-1}$. Two other IR excessive point sources (sources s03 and s05) lie immediately to either side of this source, and while resolved in *Spitzer*, all three sources are likely blended together in *ISO* images.

ISO source x02 corresponds to three different objects, two of which (x02a and x02b) are detected with *Spitzer* and show little to no IR excess despite having blue-shifted $\text{H}\alpha$ absorption cores (McDonald & van Loon 2007). The third source (x02c) is unresolved by *Spitzer*. Although apparently exhibiting a lack of IR excess, we note that x02a and x02b are located in the most dense region of the cluster where source confusion in *Spitzer* is severe and reliable photometry is difficult.

ISO source x03 is not resolved at $24 \mu\text{m}$ with MIPS, but its IRAC colors do indicate a possible (slight) $8 \mu\text{m}$ excess. The *AKARI* observation of x03 measures 3.2, 4.1, 7, and $9 \mu\text{m}$ fluxes that are four times brighter than the *Spitzer* 3.6, 4.5, and $8 \mu\text{m}$ fluxes, likely due to stellar blending in *AKARI* since x03 is located in a dense region of the cluster. Despite this discrepancy, *AKARI*

fluxes still show $x03$ to have a very slight IR excess. A strong red emission wing in the star's $H\alpha$ line and blue-shifted absorption core yield a potential mass-loss rate of $\sim 10^{-6} M_{\odot} \text{ yr}^{-1}$ (McDonald & van Loon 2007). The lack of reliable photometry redward of $8 \mu\text{m}$ prevents us from measuring a mass-loss rate in Section 3.5.

In addition to the three *ISO* sources, McDonald & van Loon (2007) obtained VLT/UVES spectra of 10 other stars in NGC 362, all of which have spectra typical for oxygen-rich red giant stars. Five of these sources show IR excess at $24 \mu\text{m}$ (see Table 2 and Section 3.5). Fitting of the $H\alpha$ profiles suggests mass-loss rates ranging from $10^{-7} - 10^{-5} M_{\odot} \text{ yr}^{-1}$. Source o01 (*Spitzer* source s06) has strong IR excess, is variable ($V16$, $P = 138$ days; Clement 1997), and shows strong molecular bands and emission in $H\alpha$.

The remaining five sources from McDonald & van Loon (2007) are also detected in IRAC. None of these sources show significant 8 or $24 \mu\text{m}$ excess, the exception being o09, which shows slight $8 \mu\text{m}$ excess ($[3.6] - [8] = 0.18$, $M_{3.6\mu\text{m}} = -5.1$ mag). It is interesting to note that all sources observed by McDonald & van Loon (2007) that show IR excess in *Spitzer* or *ISO* data also show red $H\alpha$ line emission wings. The four stars (o02, o03, o04, and o10) that have no IR excess show only blue $H\alpha$ line emission wings. McDonald & van Loon (2007) suggest that stars showing only blue emission wings have heated chromospheric material restricted to radii less than $2 R_{\odot}$, resulting in the red emission being blocked by the stellar disk. In this scenario, the chromospheres of stars showing significant IR excess will be extended to large enough radii to see a red emission in $H\alpha$.

Smith et al. (1999) obtained an optical spectrum of another NGC 362 variable from Clement (1997), V2 ($P = 90$ days). V2 is *Spitzer* source s02 (Table 2, Section 3.5.1), which has strong IR excess. Strong $H\alpha$ and $H\beta$ emission in V2 indicate chromospheric activity, and a strong $\text{Li I } \lambda 6707$ feature indicates a lithium overabundance. Low-mass giant stars have typically destroyed and diluted their photospheric lithium (which is brought to the surface via the first dredge-up), so those showing a lithium overabundance are rare, although not unheard of.

Eight sources in NGC 362 showing strong IR excess ($F_{24\mu\text{m}}/F_{7\mu\text{m}} > 1$, where zero-excess stars have $F_{24\mu\text{m}}/F_{7\mu\text{m}} \approx 0.1$) were identified by Ita et al. (2007) using *AKARI* data. These eight sources are located in the region of the IR color-magnitude diagram (CMD) that is now attributed to background galaxies (e.g., Blum et al. 2006; Boyer et al. 2008, 2009; Bolatto et al. 2007; McDonald et al. 2009), although there may also be a small amount of contamination from background evolved stars in this region. Several of the cluster members showing IR excess in *Spitzer* data are also detected by Ita et al. (2007), but these sources are not the focus of that particular study.

3.2. Identifying Mass-Losing Stars with *Spitzer*

A CMD showing *Spitzer* $[24]$ versus $[8] - [24]$ is presented in Figure 3. Confirmed non-members are represented with black dots, and sources without membership information are marked with gray dots, the majority of which are likely background galaxies. Stars on the

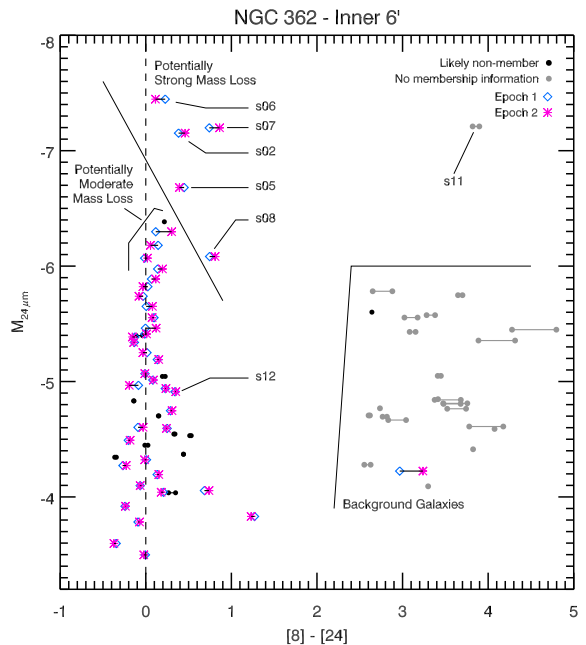


FIG. 3.— $[24]$ versus $[8] - [24]$ color-magnitude diagram. Lines connect points from each IRAC epoch. Five sources are identified as candidates of strong dusty mass-loss, and five others are candidates for moderate dusty mass loss. One of the moderately dusty candidates is a likely cluster non-member (source s01).

RGB have average colors of $[8] - [24] = 0$ mag, while stars near the bright end of the RGB begin to shift to $[8] - [24] > 0$ mag.

Table 2 lists ten sources with $[8] - [24] > 0$ mag located in the region of the CMD above or near the tip of the Red Giant Branch (TRGB; $M_{3.6\mu\text{m}} \approx -6.2$ mag, based on the drop-off in the luminosity function, shown in Figure 2). Proper motion from Tucholke (1992) indicates that source s01 is a likely non-member, but the remaining nine sources are confirmed radial velocity or proper motion cluster members. Five of the ten sources (s02, s05, s06, s07, and s08) are either very bright or have strong $24 \mu\text{m}$ excess, and we designate them as candidate strong mass-losing stars. The four more moderate confirmed member stars are potentially forming dust in smaller quantities and possibly also losing mass at a moderate rate.

In addition to the ten sources listed in Table 2, source s11 (R.A. = $1^{\text{h}}02^{\text{m}}48^{\text{s}}66$, Dec. = $-70^{\circ}45'22''6$) is very red and bright, with $[8] - [24] > 3.5$ and $M_{24\mu\text{m}} < -7$ mag. This source is the only IRAC source also detected at $70 \mu\text{m}$, and it is most likely an unresolved background galaxy, despite being more than a magnitude brighter than the general locus of other unresolved background galaxies. Its position in the $[3.6]$ versus $[3.6] - [8]$ CMD (Fig. 4) and its inferred bolometric luminosity if it were a cluster member (see Section 3.3 and Figure 7) place it among the other background galaxies, far from the mass-losing AGB stars. Moreover, this source's SED (Fig. 5) rises strongly beyond $3 \mu\text{m}$, resembling those of galaxies in the SINGS sample (e.g., Dale et al. 2006) and of other background galaxies identified in Figure 3. While we cannot confirm this source's status as a background galaxy without a spectrum or high-resolution image (S11 falls outside of the ACS field of view), we proceed under

TABLE 2
 CANDIDATE STRONG AND MODERATE MASS-LOSING STARS IN NGC 362

Source ID	R.A. (J2000) (h m s)	Dec. (J2000) ($^{\circ}$ ' ")	$M_{8\mu\text{m}}$ (mag)	$M_{24\mu\text{m}}$ (mag)	T (K)	L (L_{\odot})	Notes and Alternate Designations ^a
Moderate Mass-Loss Candidates							
s01	01 03 35.75	-70 50 52.4	-6.17 ± 0.03	-6.38 ± 0.02	3950	1656	non-member
s03	01 03 20.07	-70 50 55.0	-6.09 ± 0.03	-6.30 ± 0.02	4339	2184	o07, post-AGB?
s04	01 03 19.07	-70 50 51.1	-6.07 ± 0.03	-6.07 ± 0.03	3823	1551	x01
s09	01 03 10.67	-70 50 54.4	-6.08 ± 0.03	-6.18 ± 0.03	4226	1932	o08, post-AGB?
s10	01 02 43.34	-70 48 47.8	-5.81 ± 0.03	-5.98 ± 0.03	3975	1363	
Strong Mass-Loss Candidates							
s02	01 03 21.85	-70 54 20.2	-6.73 ± 0.03	-7.15 ± 0.02	3907	1826	V2 ($P = 90$ days)
s05	01 03 17.29	-70 50 49.1	-6.26 ± 0.05	-6.68 ± 0.02	4058	2280	o05a/o05b
s06	01 03 15.08	-70 50 31.5	-7.28 ± 0.03	-7.45 ± 0.02	3962	3106	o01, V16 ($P = 138$ days)
s07	01 03 13.62	-70 50 36.5	-6.40 ± 0.03	-7.20 ± 0.02	3343	1402	o06
s08	01 03 12.60	-70 51 00.9	-5.31 ± 0.02	-6.08 ± 0.02	3682	1842	stellar blend?

NOTE. — The prefix of the source IDs is short for “*Spitzer*”. Sources are numbered in order of decreasing R.A.
^a Designations from McDonald & van Loon (2007) have a prefix “o” or “x”, followed by a number. Source s04 (x01) was also detected by Origlia et al. (2002). Photosphere temperatures derived here for s03 and s09 are warm, possibly indicating that these are post-AGB stars. However, McDonald & van Loon (2007) estimate temperatures that place both stars firmly on the RGB.

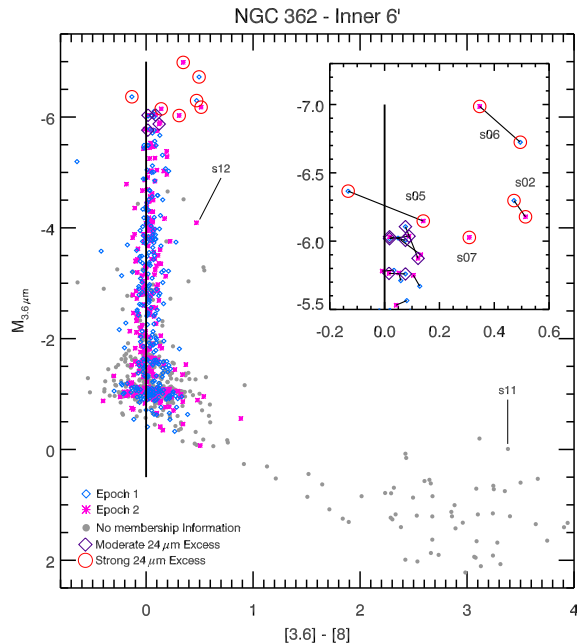


FIG. 4.— $[3.6]$ versus $[3.6] - [8]$ color-magnitude diagram. Lines connect points from each IRAC epoch. The sources identified as candidate stars with strong and moderate mass loss in Figure 3 are marked with red circles and purple diamonds, respectively. The crowded region towards the TRGB is inset at the top right. The source at $[8] - [24] > 3.5$ and $M_{24\mu\text{m}} < -7$ mag in Figure 3 (source s11) is located far from mass-losing AGB stars and near unresolved background galaxies in this CMD. Source s12 may be a background SMC carbon star.

the assumption that it is not a member of NGC 362 and exclude it from our analysis.

It is clear from the *Spitzer* data that dusty mass loss in NGC 362 is confined to the upper RGB/AGB. There are a handful of potential member stars with moderate $8\mu\text{m}$ excess at $-2 \gtrsim M_{3.6\mu\text{m}} \gtrsim -4$ mag visible in Figure 4. All of these sources are very near the cluster center, and upon visual inspection, all but one are clearly blended with other sources in all of the *Spitzer* data, potentially creating artificially red $[3.6] - [8]$ colors if the flux is not

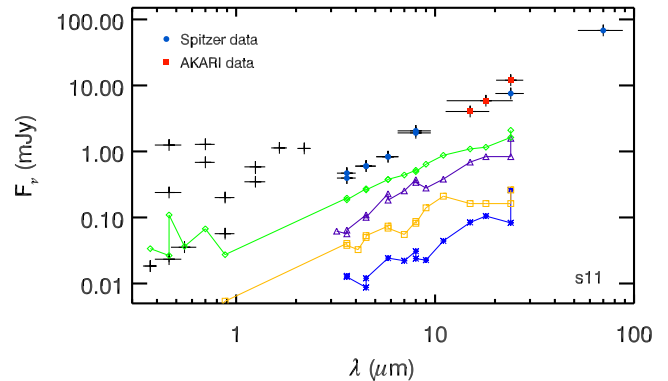


FIG. 5.— SED of source s11, a suspected background galaxy. Black pluses, blue circles, and red circles represent optical/Near-IR, *Spitzer*, and *AKARI* data, respectively. Wavelength error bars correspond to the filter widths. The scatter in the optical and near-IR photometry is likely due to mis-matching of sources, as foreground optical sources may lie directly along the sightline to the galaxy. Four other sources from the galaxy locus in Figure 3 are also shown (green diamonds, purple triangles, orange squares, and blue asterisks), plotted with offset fluxes for visual clarity. The SED of s11 resembles that of the other four background galaxies.

accurately extracted at one or both wavelengths. Indeed it is likely that the flux of these sources is inaccurate since these are only moderately bright stars located in an extremely crowded region of the cluster. Given that the mean uncertainty in their $[3.6] - [8]$ colors is 0.17 mag ($0.2 \gtrsim [3.6] - [8] \lesssim 0.3$ mag), these sources could easily be members of the non-dusty RGB.

The only potentially unblended source in this region of the CMD (s12; R.A. = $1^{\text{h}}03^{\text{m}}11^{\text{s}}59$, Dec. = $-70^{\circ}50'23''5$) is located at $[3.6] - [8] \approx 0.47 \pm 0.14$ and $M_{3.6\mu\text{m}} \approx -4$ mag in Figure 4. This source was designated a radial velocity member by Fischer et al. (1993) ($v_{\text{rad}} = 224.8$ km s^{-1}), but it has no known proper motion measurements. IR data for this source are somewhat ambiguous (Fig. 6), and it is very likely that either the IRAC photometry is inaccurate or this source is actually a background star belonging to the SMC. The source is detected at $3.6\mu\text{m}$ in only epoch two of the IRAC data,

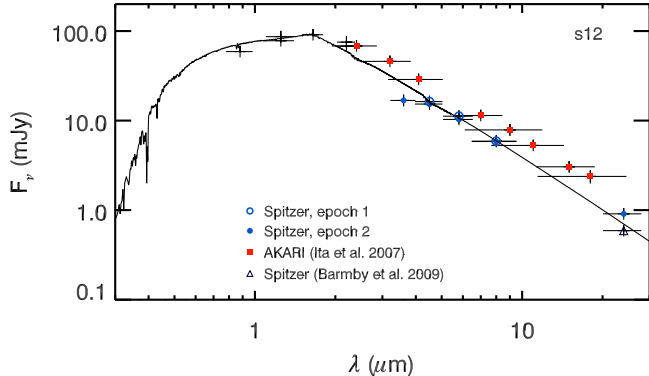


FIG. 6.— SED of source s12. The solid black line shows the best fit MARCS model (see Section 3.3). The underluminous $3.6 \mu\text{m}$ flux appears to be the cause of the $[3.6] - [8]$ excess apparent in Figure 4, and may be due to poor photometry or possibly to absorption from acetylene. *AKARI* fluxes are systematically too bright, which may be due to stellar blending.

and this flux falls well below the apparent stellar continuum, resulting in what may be an artificially red $[3.6] - [8]$ color.

Despite the under-luminous $3.6 \mu\text{m}$ flux and systematically over-luminous *AKARI* data, the SAGE-SMC $24 \mu\text{m}$ measurement of source s12 does show a very slight amount of excess. It is possible that this source may be a carbon star belonging to the SMC, and the discrepant $3.6 \mu\text{m}$ flux may indicate variability or possibly molecular absorption from acetylene (cf. van Loon et al. 2008). The heliocentric radial velocity for carbon stars on the outskirts of the SMC is $149.3 \pm 30 \text{ km s}^{-1}$, with a dispersion of $\delta v = 25.2 \pm 2.1 \text{ km s}^{-1}$ (Hatzidimitriou et al. 1997). A total of 6% of these carbon stars have velocities $200 \text{ km s}^{-1} < v_{\text{rad}} < 250 \text{ km s}^{-1}$. Given that this source has a magnitude and color very similar to typical carbon stars in the SMC (Bolatto et al. 2007), it is likely not a member of NGC 362, and, as a consequence, no significant dusty mass loss occurs below the TRGB in NGC 362.

3.3. The Hertzsprung-Russell Diagram

In Figure 7, we present a physical Hertzsprung-Russell Diagram (HRD) for NGC 362. To determine the stellar parameters of all stars in the cluster, we fit optical, near-IR, and IRAC photometry to the Model Atmosphere in Radiative and Convective Scheme (MARCS) code (Gustafsson et al. 1975, 2008). The grid of model spectra and fitting technique used here are described in more detail in McDonald et al. (2009). To fit the model spectra to the data, we give preference to MCPS photometry, including NOMAD and DENIS photometry only if a source is not present in the MCPS catalog.

A Padova isochrone (Marigo et al. 2008) is included in Figure 7 at 12.5 Gyr and $[\text{Fe}/\text{H}] = -1.28$. This metallicity is slightly lower than the $[\text{Fe}/\text{H}] = -1.16$ quoted in Harris (1996), which we use to calculate mass-loss rates in Section 3.5. We note that a value of $[\text{Fe}/\text{H}] = -1.28$ would result in a 32% increase in the gas-to-dust ratio (ψ) and therefore a 15% decrease in the dust mass loss. Also plotted are isochrones representing the SMC and distant Galactic stars. As in ω Cen (McDonald et al. 2009), the NGC 362 upper RGB is cooler than the Padova

isochrone, which may suggest (dusty or non-dusty) mass loss on the RGB. RGB mass loss is not well accounted for in Simple Stellar Population models applied to distant galaxies, but it may be of critical importance in predicting effective temperatures and thus colors and bolometric corrections (Salaris & Cassisi 2005).

The brightest/dustiest candidate mass-losing stars in the cluster are circled in red in Figure 7, and the moderately dusty stars are marked with purple diamonds. The very red source directly above the galaxy locus in Figure 3 (source s11) is underluminous and very cold on the HRD, consistent with the assertion that it is a background galaxy. Note that two of the moderately dusty sources are slightly warmer than the RGB (sources s03 and s09), which could indicate that these are post-AGB stars, although McDonald & van Loon (2007) indicated photosphere temperatures of $\approx 3900 \text{ K}$ for both stars, placing them firmly on the RGB. Source s07 is the coolest of the mass-losing stars at $T \approx 3300 \text{ K}$. McDonald & van Loon (2007) measure a temperature of $T \approx 3950 \text{ K}$, placing s07 among the other strong mass-losing stars. All other candidate mass-losing stars have typical temperatures and luminosities.

There is an anomalous source in Figure 7 with $T \approx 3700 \text{ K}$ and $L \approx 300 L_{\odot}$. If this source is at the distance of the SMC, its luminosity is $L \sim 15000 L_{\odot}$, which is typical for a carbon star. Source s12, which we suggested may also be an SMC carbon star in Section 3.2, was fit to a MARCS model with $T \approx 4800 \text{ K}$ and $L \approx 820 L_{\odot}$ (see Fig. 6). However, we note that a lack of photometry shortward of $0.9 \mu\text{m}$ for source s12 resulted in an uncertain fit.

3.4. Distribution of Dusty Stars

Figure 8 shows the spatial positions of the ten sources identified as candidate dusty mass-losing stars (including s01, a likely cluster nonmember). Within the inner $3.5'$ of the cluster, which includes all of the candidate dusty stars, confirmed cluster members are a mean distance of $1.2' \pm 0.1'$ to the cluster center. For the dusty stars, this is $0.7' \pm 0.2'$. While the dusty stars are slightly more tightly concentrated than the general population, the uncertainties easily allow for the possibility that both populations have the same central concentration, supporting the assertion that these stars are indeed cluster members.

Low-mass stars lose most of their mass on the RGB, and mass segregation will cause AGB stars to migrate to the outer regions of the cluster given that the time between the RGB and AGB phases is on the order of the relaxation time scale of NGC 362 ($\sim 10^8 \text{ yr}$; Fischer et al. 1993). However, most of the dusty stars in NGC 362 are likely RGB stars at the TRGB, and have therefore not had enough time for mass loss to alter their orbits, unless significant dustless mass loss occurred much earlier. We therefore do not expect to find that the dusty stars have orbits differing from those of the bulk population.

3.5. Mass-Loss Rates

The SEDs of the moderately dusty stars are presented in Figure 9, and the SEDs of the more extreme stars are presented in Figure 10. *AKARI* data (Ita et al. 2007) are plotted as red squares, *Spitzer* data are plotted as blue

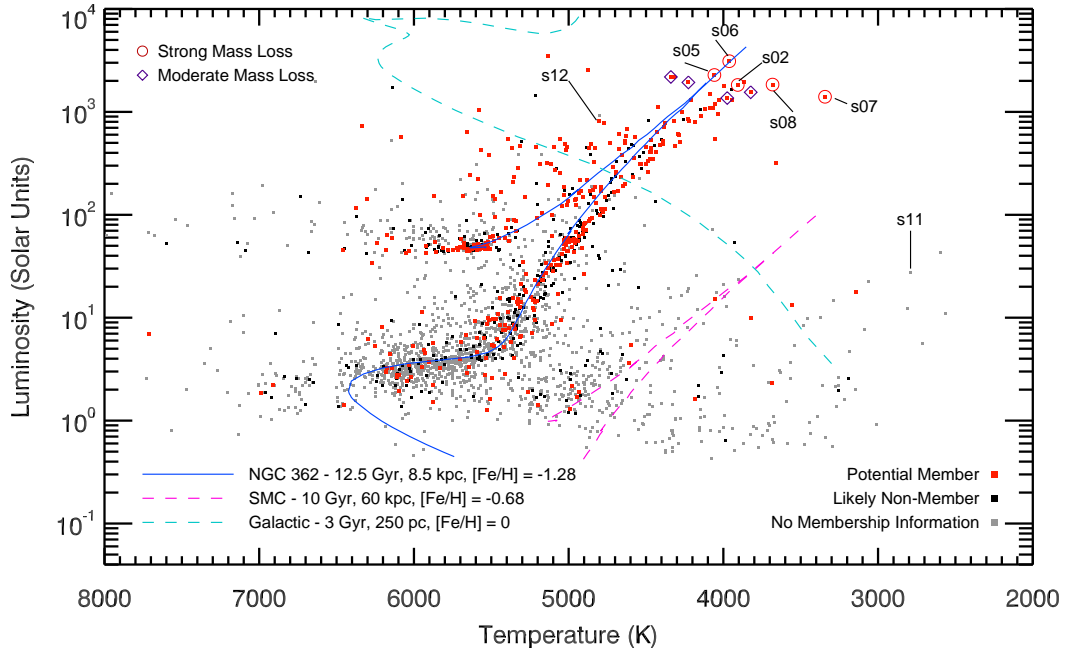


FIG. 7.— Physical HRD for NGC 362. As in Figure 4, candidate strong mass-losing stars are circled in red, and candidate moderate mass-losing stars (excluding s01, a likely cluster nonmember) are marked with purple diamonds (see Table 2). Padova isochrones are also plotted in dark blue for NGC 362, light blue (dashed line) for Galactic stars at a representative distance, and magenta (dashed line) for the SMC. Note that the RGB is cooler than expected.

circles, pluses indicate literature optical photometry, and best-fit MARCS spectra are plotted with solid lines. None of the moderate stars appears strongly variable between *Spitzer* epochs and the *AKARI* epoch (*AKARI* data for source s09 is unreliable). The extreme stars do show potential moderate variability.

The *AKARI* data for sources s09 and s07 are very inconsistent with the *Spitzer* data, which may be the result of source confusion in *AKARI*. Without exception, *AKARI* 24 μm fluxes are bright compared to *Spitzer* 24 μm photometry. This discrepancy is probably due to the poor angular resolution of *AKARI* compared to *Spitzer* (see Section 2.1), resulting in source confusion and blending. All but three of the sources in Table 2 were also detected at 24 μm by Barmby et al. (2009). These 24 μm data are very consistent with the *Spitzer* SAGE-SMC 24 μm data, typically differing by a tenth of a magnitude or less. Source s02 is the only exception to this, with a difference of 0.5 mag between *Spitzer* SAGE-SMC and Barmby et al. (2009).

To estimate the mass-loss rates, we fit the SEDs using the DUSTY modeling code (Nenkova et al. 1999). Following McDonald et al. (2009), the SEDs are fit by models using dust composed of either amorphous carbon (AMC, Hanner 1988) or silicates, with the latter composed of 65% astronomical silicates (Draine & Lee 1984), 15% compact Al_2O_3 (optical constants from the Jena database⁸), and 10% each of glassy and crystalline silicates (Jäger et al. 1994). These two dust compositions result in good fits, but the dust may consist of other silicate or carbon species or different proportions of species. Carbonaceous dust yields relatively blue [8] – [24] colors,

whereas oxygen-rich dust always produces a relatively large 24 μm excess compared to 8 μm , although without *AKARI* data to fill the gap between 8 and 24 μm left by *Spitzer*, it is difficult to definitively distinguish between different dust compositions.

Following McDonald et al. (2009), the resulting mass-loss rates from DUSTY were converted to real mass-loss rates using the following prescription, which implicitly assumes a scaling of the wind speed based upon a dust-driven wind formalism:

$$\dot{M}_{\text{dust}} = \frac{\dot{M}_{\text{DUSTY}}}{200} \left(\frac{L}{10^4} \right)^{3/4} \left(\frac{\psi}{200} \right)^{-1/2} \left(\frac{\rho_d}{3} \right)^{1/2} \quad (1)$$

$$\dot{M}_{\text{gas}} = \psi \dot{M}_{\text{dust}}, \quad (2)$$

where ψ is the gas-to-dust ratio ($\psi = 2891$, assuming $[\text{Fe}/\text{H}] = -1.16$ and $\psi_{\odot} = 200$), L is the stellar luminosity determined from the MARCS best fit, and ρ_d is the bulk grain density. For silicates, we assume $\rho_d = 3 \text{ g cm}^{-3}$, and for AMC grains, we assume $\rho_d = 2.5 \text{ g cm}^{-3}$. Note that a decrease in metallicity to $[\text{Fe}/\text{H}] = -1.28$ would result in a 15% decrease in \dot{M}_{dust} . A summary of input model parameters and output mass-loss rates is presented in Table 3.

The moderately dusty stars are all fit well by silicate dust. In addition, source s09 is fit equally well by AMC dust due to a lack of reliable *AKARI* data. The mass-loss rate for s09 from the best-fit AMC model is a factor of 1.7 less than the rate from the best-fit silicate model. Together, the four moderately dusty cluster members lose $\dot{M}_{\text{dust}} = 8.3(\pm 0.6) \times 10^{-10} M_{\odot} \text{ yr}^{-1}$, where the errors come solely from the dust composi-

⁸ <http://www.astro.uni-jena.de/Users/database/entry.html>

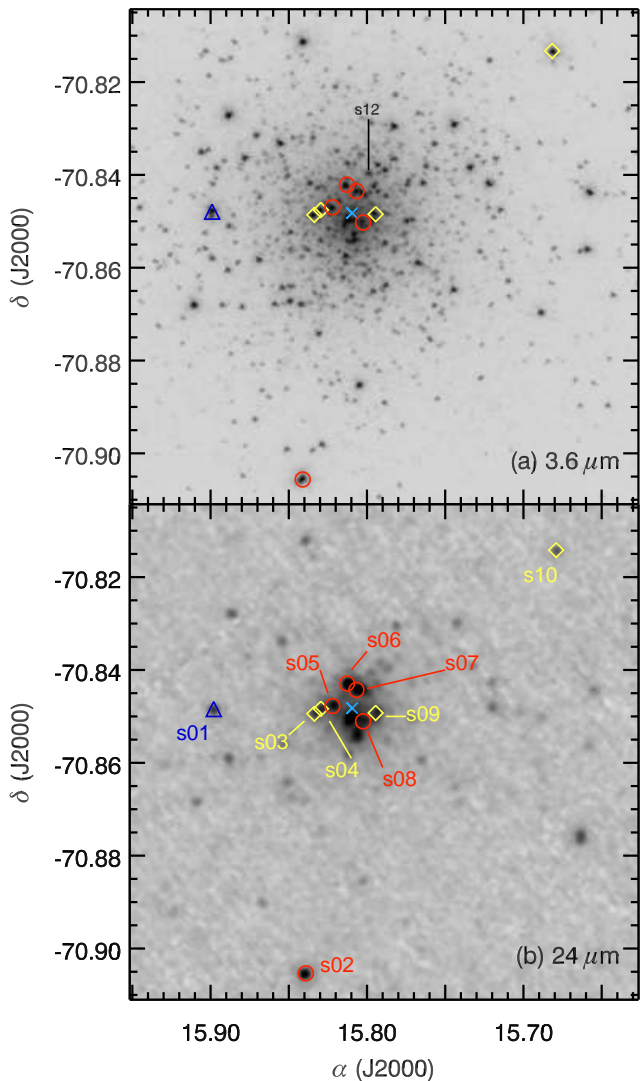


FIG. 8.— Distribution of candidate mass-losing stars. Most dusty stars are located within the inner $1'$ of the cluster center. Red circles mark sources with strong mass loss, and yellow diamonds mark sources experiencing moderate mass loss. The open blue triangle (source s01) is a likely cluster non-member. Source s11, a background galaxy, falls well outside the field of view shown here. tion used for source s09. This corresponds to $\dot{M}_{\text{gas}} = 2.4(\pm 0.2) \times 10^{-6} M_{\odot} \text{ yr}^{-1}$.

It is not surprising to find silicate dust in the outflows of these four moderate stars. Höfner & Andersen (2007) and Höfner (2008) suggest that winds could be driven by large ($\sim 1 \mu\text{m}$) Fe-free silicate grains, or that silicates can easily form in winds that are driven by carbon grains.

3.5.1. The most extreme dust producers

Five sources are classified as strong mass-losing stars (s02, s05, s06, s07, and s08). We do not attempt to fit a DUSTY model to source s08 due to inconsistent *Spitzer* and optical photometry and a lack of *AKARI* photometry (Fig. 11). The remaining four stars do appear moderately variable in the IR between *Spitzer* and *AKARI* epochs (Fig. 10), with s05 showing the largest amplitude followed by s02 and s06, which are the known variable stars V2 and V16, respectively. The total dust-traced mass-loss rate from the four extreme stars is $\dot{M}_{\text{gas}} = 6.2(\pm 0.5) \times 10^{-6} M_{\odot} \text{ yr}^{-1}$, with the uncertainty

TABLE 3
MASS-LOSS RATES

Source ID	T_{inner} (K)	Dust Type	\dot{M}_{dust} ($M_{\odot} \text{ yr}^{-1}$)	\dot{M}_{gas} ($M_{\odot} \text{ yr}^{-1}$)
s02	500	AMC	5.9×10^{-10}	1.7×10^{-6}
s03	1200	silicate	2.5×10^{-10}	7.1×10^{-7}
s04	1200	silicate	2.1×10^{-10}	6.1×10^{-7}
s05 ^a	1000	silicate	3.2×10^{-10}	9.3×10^{-7}
s06	600	AMC	7.0×10^{-10}	2.0×10^{-6}
s07	800	silicate	4.6×10^{-10}	1.3×10^{-6}
s09 ^b	1200	silicate	2.6×10^{-10}	7.4×10^{-7}
s10	1200	silicate	1.7×10^{-10}	4.8×10^{-7}

NOTE. — Sources s02 and s06 are fit equally well to a DUSTY model composed of a combination of silicates and AMC dust, resulting in a nearly identical mass-loss rate to that derived from the AMC models. See Section 3.5.2 for a description of the uncertainties in the mass-loss rates quoted here.

^a The silicate model fits well to the *Spitzer* data for s05. *AKARI* data for s05 is better fit by an AMC model with $T_{\text{inner}} = 800$ K, $\dot{M}_{\text{dust}} = 5.6 \times 10^{-10} M_{\odot} \text{ yr}^{-1}$, and $\dot{M}_{\text{gas}} = 1.6 \times 10^{-6} M_{\odot} \text{ yr}^{-1}$.

^b Source s09 is fit equally well to a model with AMC dust and $T_{\text{inner}} = 800$ K. The resulting mass-loss rates are a factor of 1.7 less than the rates derived from the silicate model.

depending on the dust compositions chosen. This is more than twice the contribution of the four more moderate stars.

The dust composition is difficult to estimate for the four extreme sources. Source s05 is particularly odd. The *AKARI* and *Spitzer* data appear to show two different dust compositions. AMC dust fits best to the *AKARI* data, but is simultaneously ruled out by the *Spitzer* data due to a lack of excess between 3.6 and 8 μm . McDonald & van Loon (2007) found that this source is actually two stars (o05a/o05b) with similar temperatures and luminosities ($T \approx 4100$ K, $L_{\text{o05a}} = 2103 \pm 189 L_{\odot}$, $L_{\text{o05b}} = 2392 \pm 213 L_{\odot}$), which are totally unresolved in both *Spitzer* and *AKARI* data. Both stars appear oxygen-rich and show blue-shifted $\text{H}\alpha$ absorption cores that indicate an outflow of material. It is unclear how their small separation ($0.2''$) has affected the IR photometry. It is possible that the low resolution of the *AKARI* images has resulted in blending of sources in addition to o05a and o05b, causing inflated *AKARI* fluxes. Another possibility is that one or both of these sources is variable, producing different types of dust in varying proportions during different phases of the pulsation cycle. A third possibility is that neither star has a real IR excess, and the apparent excess is caused by inaccurate flux extraction due to stellar blending in this crowded region of the cluster. However, this third possibility seems unlikely since s05 also shows a strong 24 μm excess (Fig. 10), suggesting that at least one of the stars is producing dust. Nevertheless, the $\text{H}\alpha$ line clearly shows that both stars (o05a/o05b) are losing mass, although it may not be as clear that the mass loss in either star is accompanied by dust production.

For source s07, *AKARI* photometry is available only at 24 μm , and this flux is more than twice the flux measured with MIPS at 24 μm . If the *AKARI* 24 μm flux is accurate, it can only be explained by an extremely large quantity of circumstellar dust. This, along with the

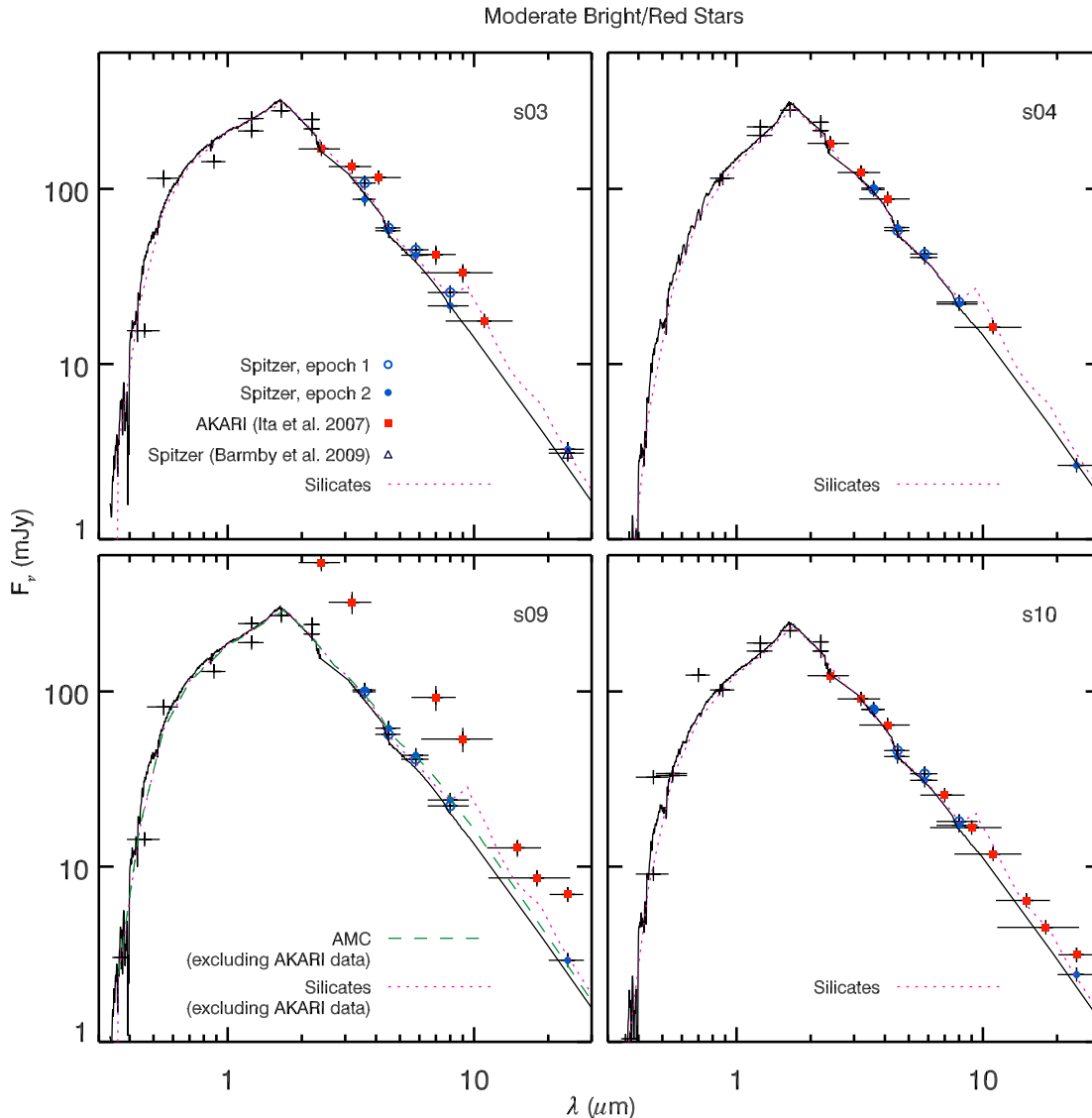


FIG. 9.— SEDs of moderately dusty stars at the TRGB in NGC 362. Wavelength error bars correspond to the filter width. *AKARI* data are plotted as red squares and *Spitzer* data are plotted as blue circles. MARCS models are solid black lines. IRAC epoch 1 is plotted with open blue circles, and IRAC epoch 2 is plotted with closed blue circles. All four stars are well fit by a DUSTY silicate model (magenta, dotted line), but s09 is fit equally well by a DUSTY amorphous carbon (AMC) model (green, dashed line).

source’s location near several other bright $24\ \mu\text{m}$ sources, suggests that the *AKARI* $24\ \mu\text{m}$ flux is overestimated. We therefore exclude the *AKARI* $24\ \mu\text{m}$ point from the DUSTY fit and find that silicate dust provides the best fit due to the lack of strong excess in the IRAC data.

The two remaining extreme sources, s02 (V2) and s06 (V16/o01), are the most extreme stars in the cluster and exhibit the strongest mass-loss rates. Neither star is fit well by silicates alone, but both are well fit by AMC models. This is surprising, given that the optical spectrum of s06 indicates $\text{C}/\text{O} < 1$ (McDonald & van Loon 2007). Smith et al. (1999) did not measure the carbon abundance in star s02, so its nature as carbon or oxygen-rich remains unknown. Carbon stars are known to reside in GCs, notably in ω Cen (van Loon et al. 2007). Models that include a combination of 50% AMC dust and 50% silicate dust also fit well to both s06 and s02, but we note that to fit this model to s02, we must exclude the

AKARI photometry, which shows no silicate features.

A mid-IR spectrum of s02 was obtained by Y. Ita et al. (in preparation) using *AKARI* IRC slit-less spectroscopy. Pre-analysis of the spectrum suggests a complete lack of silicates and the possible presence CO and water absorption near 3 and $5\ \mu\text{m}$, which may explain the underluminous *AKARI* photometry near these wavelengths. While we cannot definitively declare a dust type in either s02 or s06, AMC dust must play some role if we are to reconcile the strong photometric excess in the IRAC bands and the excess at $24\ \mu\text{m}$.

3.5.2. Uncertainties in the Mass-Loss Rates

The uncertainties quoted for the total mass-loss rates of the candidate mass-losing stars reflect a range of values that depends on the dust composition chosen. The uncertainties in the mass-loss rates for individual stars is not reflected in this value. In ω Cen, uncertainties of

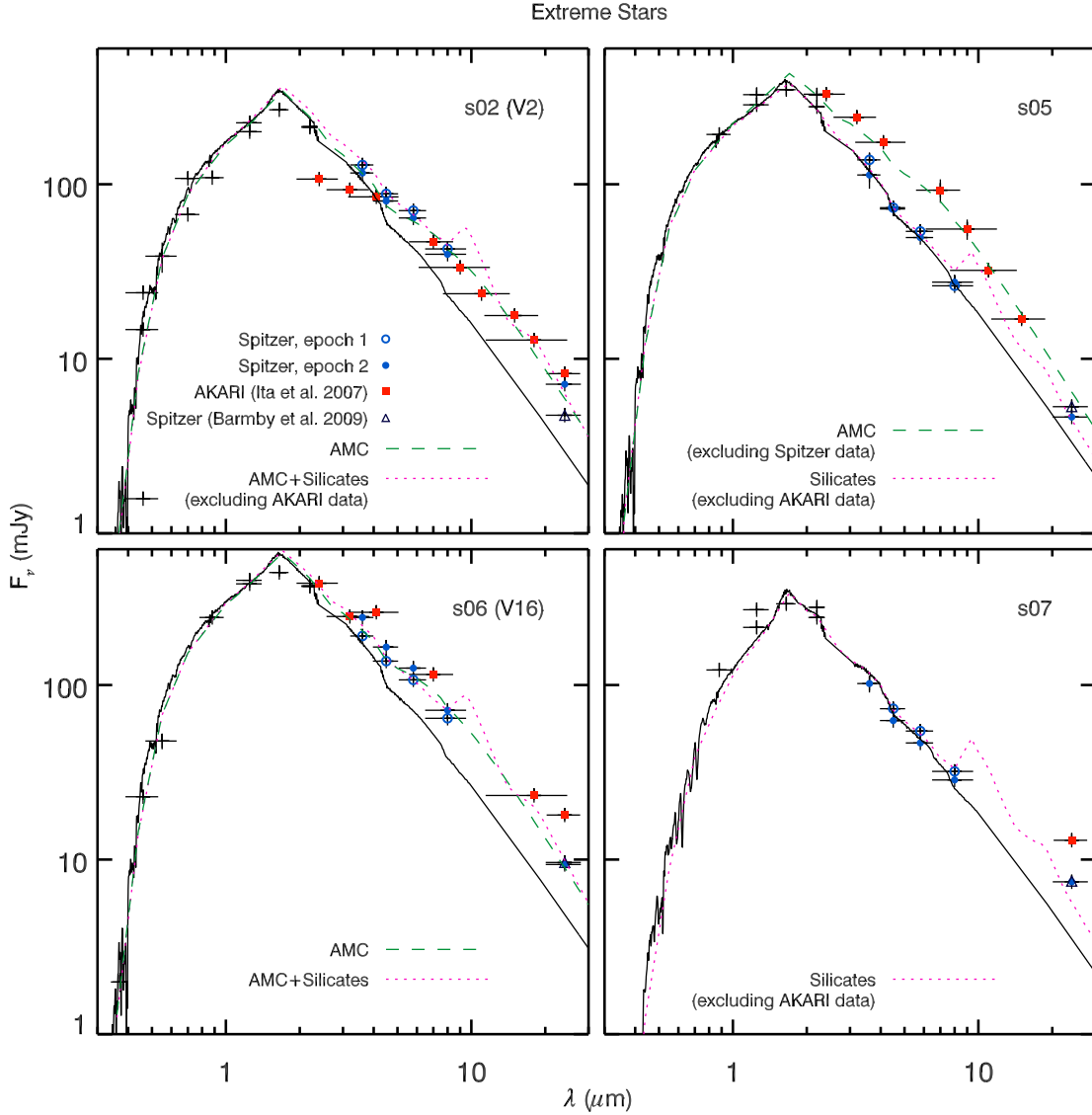


FIG. 10.— Same as Figure 9, but for the most extreme stars in NGC 362. The amorphous carbon (AMC) + silicate DUSTY models shown for s02 and s06 are a combination of 50% AMC and 50% silicates.

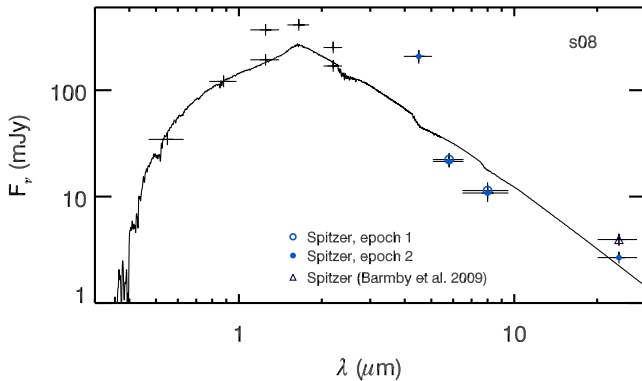


FIG. 11.— SED for source s08. We did not attempt to fit a DUSTY model to this SED due to inconsistent *Spitzer* and optical photometry and a lack of *AKARI* photometry. This source may be affected by stellar blending or it may be extremely variable.

ual stars, based on internal errors from DUSTY and on several assumptions. These assumptions include (1) pulsation causes only negligible variations in the mid-IR, (2) the gas-to-dust ratio scales with metallicity, (3) the wind velocity scales as $v_{\text{wind}} \propto L^{1/4}(\psi)^{-1/2}$, and (4) dust-to-gas coupling is efficient. See McDonald et al. (2009) for a more detailed discussion of mass-loss rate uncertainties.

We note that the prescription we use to estimate the mass-loss rates assumes that the wind speed scales as $v_{\text{wind}} \propto L^{1/4}(\psi\rho_d)^{-1/2}$, resulting in velocities ranging from $v_{\text{wind}} = 0.5 - 1.3 \text{ km s}^{-1}$ for mass-loss candidates in NGC 362. These small velocities provide the largest uncertainty to our mass-loss rates, as they are on the order of the turbulence in the wind ($\sim 1 - 2 \text{ km s}^{-1}$; Schöier et al. 2004). It is not clear whether very slow winds can be sustained, but it is possible that wind speeds can be increased to $\lesssim 10 \text{ km s}^{-1}$ due to the effects of rotation and pulsation in the star. Moreover, McDonald & van Loon (2007) estimated that the

52 – 80% were derived for the mass-loss rates of individ-

wind velocities in several NGC 362 stars range from $\approx 6 - 17 \text{ km s}^{-1}$. If these velocities are good approximations of the wind speed in the dust-producing zone, then the mass-loss rates of each star will increase by up to a factor 6.

4. DISCUSSION

4.1. Dust and Mass Loss in V2 and V16

Star s06 (V16) appears to show carbon dust despite its nature as an oxygen-rich star. Star s02 (V2) is similar, although its nature as carbon- or oxygen-rich is unknown. These stars are akin to V42 in ω Cen (cf. McDonald et al. 2009), an oxygen-rich star which once may have shown a strong $10\text{-}\mu\text{m}$ silicate dust feature, but more recently appears to show predominantly amorphous carbon dust despite its oxygen-rich atmosphere. While ω Cen V42 and NGC 362 V16 both appear to be currently dominated by carbonaceous dust, they may still contain some (possibly variable) amounts of silicates. 47 Tuc is home to two dusty stars (V1 and V18) that show variable silicate emission (van Loon et al. 2006a; Lebzelter et al. 2006). Höfner & Andersen (2007) suggest a possible scenario where non-local thermodynamic equilibrium conditions allow the periodic production of different grain compositions at different epochs in the pulsation cycle. It may also be the case that grain size varies enough that large grains periodically suppress the silicate features.

4.2. Global Mass Loss

The cluster stars that exhibit IR excesses are currently returning $\dot{M}_{\text{gas}} = 8.6^{+5.6}_{-3.4} \times 10^{-6} M_{\odot} \text{ yr}^{-1}$ of gas to the ICM, using the same fractional errors used in McDonald et al. (2009). To find the total cluster mass loss (dusty and dustless), we estimate the mass-loss rates for non-dusty stars using the method described in Schröder & Cuntz (2005), which is based on the stellar temperature and luminosity. We find that chromospherically-driven (dustless) mass loss is responsible for $2 \times 10^{-6} M_{\odot} \text{ yr}^{-1}$, giving a total cluster mass loss of $\dot{M}_{\text{total}} \approx 1.1^{+0.7}_{-0.4} \times 10^{-5} M_{\odot} \text{ yr}^{-1}$. Dust production therefore accompanies 80% of the current mass loss in NGC 362.

The global mass-loss rate for NGC 362 is virtually identical to that of ω Cen ($\approx 1.2 \times 10^{-5} M_{\odot} \text{ yr}^{-1}$; McDonald et al. 2009), despite NGC 362 being an order of magnitude less massive than the latter. 47 Tuc, which is similar in mass to ω Cen, appears to have a similar global mass-loss rate, given that its four long-period variables have mass-loss rates ranging from 10^{-7} to $10^{-6} M_{\odot} \text{ yr}^{-1}$ (Origlia et al. 2007). In all three clusters, only a handful of stars are dominating the global mass-loss rate. This supports the likelihood that global dust production and dust-associated mass loss in clusters are stochastic in nature, driven by episodic dust production in the individual stars (possibly due to varying stellar conditions at different pulsation phases) and the rarity of the stars themselves. ω Cen may currently be experiencing a relatively quiescent period of dust production, given that only two stars (V6 and V42) are currently forming significant amounts of dust. M15, on the other hand, appears to have recently experienced a period of strong dust production, assuming that the ICM dust present there was formed in stellar winds rather

than by a stellar collision (Rasio & Shapiro 1991) or one or more diffusing planetary nebulae. NGC 362 has a moderate total mass ($3.78 \times 10^5 M_{\odot}$) and up to four stars producing significant amounts of dust. NGC 362 may therefore be representative of a more intermediate phase of dust production in the typical GC.

Any effects that metallicity has on dust production appear to be overshadowed by the apparent episodic nature of dust production. Stars with strong IR excess are discovered in clusters with metallicities ranging from $[\text{Fe}/\text{H}] = -2.4$ for M15 (e.g., Boyer et al. 2006) to $[\text{Fe}/\text{H}] = -0.7$ for 47 Tuc (van Loon et al. 2006a), with no clear trend favoring higher metallicities.

Dust production is dominated by the most luminous stars in the cluster. However, several dustless stars have temperatures and luminosities similar to the dust-producing stars. The $\text{H}\alpha$ profiles of at least a handful of these dustless stars suggest that they are losing mass without any associated dust production. The only observed difference known to exist between the dusty and non-dusty stars is a lack of a red $\text{H}\alpha$ line emission wing in the non-dusty stars, perhaps suggesting that material is restricted to smaller stellar radii than in the dusty stars (cf. McDonald & van Loon 2007).

4.3. The Intracluster Medium

If we make the (possibly naïve) assumption that the rate of gas return has remained relatively constant since NGC 362 last plunged through the Galactic plane (3×10^7 yr ago), then we might expect $210 - 540 M_{\odot}$ of gas and $0.05 - 0.15 M_{\odot}$ of dust to have gathered in the ICM, especially considering that the cluster escape velocity is much larger than typical wind speeds derived with DUSTY ($v_{\text{esc},0} = 46.7 \text{ km s}^{-1}$, $v_{\text{wind}} = 0.5 - 1.3 \text{ km s}^{-1}$, assuming $v_{\text{wind}} \propto L^{1/4}(\psi\rho_d)^{-1/2}$). Rotation and magnetic activity and pulsation shocks can increase wind velocity by up to an order of magnitude (cf. Bowen 1988), but this increase is still not sufficient for material to escape the cluster. Within the half-light radius, upper limits of only $< 6.3 \times 10^{-5} M_{\odot}$ of dust (Barmby et al. 2009) and $< 1.8 M_{\odot}$ of ionized hydrogen (Hesser & Shawl 1977) have been determined in the ICM of NGC 362.

Assuming that $\lesssim 5\%$ of the ICM gas is ionized, as in 47 Tuc (Smith et al. 1990; Freire et al. 2001), we find that there is $< 40 M_{\odot}$ of neutral gas in the ICM of NGC 362. Based on the total (dust + dustless) cluster mass-loss rate ($1.1 \times 10^{-5} M_{\odot} \text{ yr}^{-1}$), we can expect neutral gas to be cleared from the cluster on timescales $< 3.6 \times 10^6$ yr, more than an order of magnitude shorter than the time since the last Galactic plane-crossing. The dust provides an even shorter timescale of ICM removal or destruction, namely $< 2 \times 10^4$ yr, given a dust mass-loss rate of $3 \times 10^{-9} M_{\odot} \text{ yr}^{-1}$ and a dust upper limit of $< 6.3 \times 10^{-5} M_{\odot}$. To escape the half-mass radius ($0.81'$) within 20 000 yr, the dust would have to travel $> 80 \text{ km s}^{-1}$. This velocity is much higher than the likely wind velocities ($v_{\text{wind}} \lesssim 10 \text{ km s}^{-1}$, McDonald & van Loon 2007; Mészáros et al. 2009), requiring that (a) either the dust is dissociated on short timescales within the cluster or that (b) dust is rapidly accelerated out of the cluster.

Based on the space velocity of NGC 362, (140 km s^{-1} , cf. Odenkirchen et al. 1997), ram-pressure from hot

Galactic Halo gas could clear the cluster ICM in $\approx 2.8 \times 10^5$ yr. A stellar collision has enough kinetic energy to clear the ICM, and such collisions occur on timescales of $\approx 2.5 \times 10^6$ yr in NGC 362 (cf. Barmby et al. 2009). If ICM *dust* were destroyed within the cluster on the required shorter timescales, then ram-pressure stripping or a stellar collision may be responsible for the lack of gas and the byproducts of dust destruction in NGC 362.

Although mass loss estimates predict the presence of $\sim 10^2 M_\odot$ of ICM material in most GCs, nothing approaching this amount of mass has ever been observed. ω Cen has an upper limit of $< 10^{-4} M_\odot$ of dust (Boyer et al. 2008) and $< 2.8 M_\odot$ of neutral gas (Smith et al. 1990). Barmby et al. (2009) finds ICM dust mass upper limits of $< 10^{-4} M_\odot$ in eight GCs, and Matsunaga et al. (2008) finds upper limits of $< 10^{-3} M_\odot$ of dust in 12 GCs. van Loon et al. (2009) determined 3σ upper limits between 6 and $51 M_\odot$ of neutral hydrogen within the tidal volumes of four GCs. Much of the ICM may be ionized, as demonstrated in 47 Tuc, where up to $0.1 M_\odot$ of ionized gas was discovered (Freire et al. 2001). M15 shows the strongest evidence for an ICM, with firm detections of $9 \times 10^{-4} M_\odot$ of dust (Boyer et al. 2006) and $0.3 M_\odot$ of neutral hydrogen (van Loon et al. 2006b). The combination of episodic dust production and a stochastic ICM removal process (such as a stellar collision) could explain the lack of dusty ICM material in GCs and its unusual presence in M15. If ram-pressure stripping from hot Halo gas is the dominant removal mechanism, the intense crowding in M15 ($\log(r_{\text{tidal}}/r_{\text{core}}) = 2.5$, compared to 1.9 for NGC 362; Harris 1996) could cause the stripping of material in the center of the cluster to be less efficient, with bow-shocks around outer stars effectively shielding the cluster's ICM.

It has become clear that low-mass, low-metallicity stars successfully form dust and lose mass. Therefore, some mechanism must remove gas and dust from GCs. This material may ultimately reside in the Galactic Halo, fall back onto cluster stars, or find its way back into the Milky Way disk (e.g., Evans et al. 2003; Boyer et al. 2006; van Loon et al. 2006b, 2009). In any case, low-

mass, low-metallicity stars like those in globular clusters must collectively and continuously contribute a large amount of recycled and enriched material to the ISM, helping to drive galaxy evolution.

5. SUMMARY OF RESULTS AND CONCLUSIONS

We present an analysis of dusty mass loss in the Galactic globular cluster NGC 362 carried out with data serendipitously obtained during *Spitzer* SAGE-SMC observations of the Small Magellanic Cloud. Spectral energy distribution modeling of all cluster stars provided stellar parameters, allowing the construction of a physical Hertzsprung-Russell Diagram. The Red Giant Branch (RGB) is slightly cooler than the Padova isochrone, indicating significant mass loss on the RGB.

Significant infrared (IR) excess exists only at and above the tip of the RGB. The four brightest stars at $24 \mu\text{m}$ exhibit the strongest IR excess. Four additional stars near the tip of the RGB show moderate IR excess. Modeling with the DUSTY code indicates that these eight stars contribute $8.6^{+5.6}_{-3.4} \times 10^{-6} M_\odot \text{ yr}^{-1}$ of gas and $3.0^{+2.0}_{-1.2} \times 10^{-9} M_\odot \text{ yr}^{-1}$ of dust to the intracluster medium. The two most extreme stars, variables V2 and V16, provide up to 45% of the total (dust accompanied) mass loss.

The eight dustiest stars show evidence of silicate dust, but, surprisingly, three of the four more extreme stars require some amount of amorphous carbon dust to explain their mid-IR excesses. Strong mass loss therefore appears to correlate with a larger contribution from carbon dust, which may suggest that non-equilibrium conditions are common in such stars.

We thank Jay Anderson for sharing the Hubble ACS image and Yoshifusa Ita for sharing *AKARI* photometry and the mid-IR spectrum of star s02. We also thank the referee for his or her helpful comments. This work was supported by *Spitzer* via JPL contracts 1309827 and 1340964.

REFERENCES

- Barmby, P., Boyer, M. L., Woodward, C. E., Gehrz, R. D., van Loon, J. Th., Fazio, G. G., Marengo, M., & Polomski, E. 2009, *AJ*, 137, 207
- Blum, R. D., et al. 2006, *AJ*, 132, 2034
- Bolatto, A. D., et al. 2007, *ApJ*, 655, 212
- Bowen, G. H. 1988, *ApJ*, 329, 299
- Bellazzini, M., Fusi Pecci, F., Ferraro, F. R., Galletti, S., Catelan, M., & Landsman, W. B. 2001, *AJ*, 122, 2569
- Boyer, M. L., McDonald, I., van Loon, J. Th., Woodward, C. E., Gehrz, R. D., Evans, A., Dupree, A. K. 2008, *AJ*, 135, 1395
- Boyer, M. L., Skillman, E. D., van Loon, J. Th., Gehrz, R. D., & Woodward, C. E. 2009, *ApJ*, 697, 1993
- Boyer, M. L., Woodward, C. E., van Loon, J. Th., Gordon, K. D., Evans, A., Gehrz, R. D., Helton, L. A., & Polomski, E. F. 2006, *AJ*, 132, 1415
- Catelan, M., Bellazzini, M., Landsman, W. B., Ferraro, F. R., Fusi Pecci, F., & Galletti, S. 2001, *AJ*, 122, 3171
- Clement, C. M. 1997, *VizieR On-line Data Catalog V/97*, original catalog published in Sawyer Hogg H. 1973, *PDDO*, 3, 6
- Dale, D. A., et al. 2006, *ApJ*, 646, 161
- Draine, B. T., & Lee, H. M. 1984, *ApJ*, 285, 89
- Epchtein, N., et al. 1997, *The Messenger*, 87, 27
- Evans, A., Stickel, M., van Loon, J. Th., Eyres, S. P. S., Hopwood, M. E. L., & Penny, A. J. 2003, *A&A*, 408, L9
- Fischer, P., Welch, D. L., Mateo, M., & Côté, P. 1993, *AJ*, 106, 1508
- Fraix-Burnet, D., Davoust, E., & Charbonnel, C. 2009, *MNRAS*, in press
- Freire, P. C., Kramer, M., Lyne, A. G., Camilo, F., Manchester, R. N., & D'Amico, N. 2001, *ApJ*, 557, L105
- Gehrz, R. 1989, *Interstellar Dust*, 135, 445
- Gehrz, R. D., et al. 2007, *Review of Scientific Instruments*, 78, 011302
- Gnedin, O. Y., & Ostriker, J. P. 1997, *ApJ*, 474, 223
- Grindlay, J. E., & Liller, W. 1977, *ApJ*, 216, L105
- Gustafsson, B., Bell, R. A., Eriksson, K., & Nordlund, Å. 1975, *A&A*, 42, 407
- Gustafsson, B., Edvardsson, B., Eriksson, K., Jørgensen, U. G., Nordlund, Å., & Plez, B. 2008, *A&A*, 486, 951
- Hanner, M. 1988, *Technical Report, Optical Grain Properities*. *Washington*, p.22
- Harris, W. E. 1996, *VizieR Online Data Catalog*, 7195, 0
- Harris, J., & Zaritsky, D. 2006, *AJ*, 131, 2514
- Hatzidimitriou, D., Croke, B. F., Morgan, D. H., & Cannon, R. D. 1997, *A&AS*, 122, 507
- Hesser, J. E., & Shawl, S. J. 1977, *ApJ*, 217, L143
- Höfner, S., & Andersen, A. C. 2007, *A&A*, 465, L39
- Höfner, S. 2008, *A&A*, 491, L1

- Ita, Y., et al. 2007, PASJ, 59, 437
- Jäger, C., Mutschke, H., Begemann, B., Dorschner, J., & Henning, T. 1994, A&A, 292, 641
- Lebzelter, T., Posch, T., Hinkle, K., Wood, P. R., & Bouwman, J. 2006, ApJ, 653, L145
- Marigo, P., Girardi, L., Bressan, A., Groenewegen, M. A. T., Silva, L., & Granato, G. L. 2008, A&A, 482, 883
- Matsunaga, N., et al. 2008, PASJ, 60, 415
- Mészáros, Sz., Avrett, E. H., Dupree, A. K. 2009, AJ, 138, 615
- Meixner, M., et al. 2006, aj, 132, 2268
- McDonald, I., & van Loon, J. Th. 2007, A&A, 476, 1261
- McDonald, I., van Loon, J. Th., Decin, L., Boyer, M. L., Woodward, C. E., Gehrz, R. D., Evans, A., & Dupree, A. K. 2009, MNRAS, 394, 831
- McLaughlin, D. E., & van der Marel, R. P. 2005, ApJS, 161, 304
- Murakami, H., et al. 2007, PASJ, 59, 369
- Nenkova, M., Ivezić, Ž., & Elitzur, M. 1999, LPI Contributions, 969, 20
- Odenkirchen, M., Brosche, P., Geffert, M., & Tucholke, H. J. 1997, New Astronomy, 2, 477
- Onaka, T., et al. 2007, PASJ, 59, S401
- Origlia, L., Ferraro, F. R., Fusi Pecci, F., & Rood, R. T. 2002, ApJ, 571, 458
- Origlia, L., Rood, R. T., Fabbri, S., Ferraro, F. R., Fusi Pecci, F., & Rich, R. M. 2007, ApJ, 667, L85
- Rasio, F. A., & Shapiro, S. L. 1991, ApJ, 377, 559
- Salaris, M., & Cassisi, S. 2005, Evolution of Stars and Stellar Populations, by Maurizio Salaris, Santi Cassisi, pp. 400. ISBN 0-470-09220-3. Wiley-VCH, December 2005
- Sarajedini, A., et al. 2007, AJ, 133, 1658
- Schöier, F. L., Olofsson, H., Wong, T., Lindqvist, M., & Kerschbaum, F. 2004, A&A, 422, 651
- Schröder, K.-P., & Cuntz, M. 2005, ApJ, 630, L73
- Skrutskie, M. F., et al. 2006, AJ, 131, 1163
- Smith, G. H., Wood, P. R., Faulkner, D. J., & Wright, A. E. 1990, ApJ, 353, 168
- Smith, V. V., Shetrone, M. D., & Keane, M. J. 1999, ApJ, 516, L73
- Tucholke, H. J. 1992, A&AS, 93, 311
- van Loon, J. Th., Cohen, M., Oliveira, J. M., Matsuura, M., McDonald, I., Sloan, G. C., Wood, P. R., & Zijlstra, A. A. 2008, A&A, 487, 1055
- van Loon, J. Th., McDonald, I., Oliveira, J. M., Evans, A., Boyer, M. L., Gehrz, R. D., Polomski, E., & Woodward, C. E. 2006a, A&A, 450, 339
- van Loon, J. Th., Stanimirović, S., Evans, A., & Muller, E. 2006b, MNRAS, 365, 1277
- van Loon, J. Th., Stanimirović, S., Putman, M. E., Peek, J. E. G., Gibson, S. J., Douglas, K. A., & Korpela, E. J. 2009, MNRAS, 396, 1096
- van Loon, J. Th., van Leeuwen, F., Smalley, B., Smith, A. W., Lyons, N. A., McDonald, I., & Boyer, M. L. 2007, MNRAS, 382, 1353
- Werner, M. W., et al. 2004, ApJS, 154, 1
- Zacharias, N., Monet, D. G., Levine, S. E., Urban, S. E., Gaume, R., & Wycoff, G. L. 2005, VizieR Online Data Catalog, 1297, 0
- Zaritsky, D., Harris, J., Thompson, I. B., Grebel, E. K., & Massey, P. 2002, AJ, 123, 855